Published in final edited form as:
J Immunol. 2015 March 1; 194(5): 2345–2357. doi:10.4049/jimmunol.1402350.

Macrophage mitochondrial and stress response to ingestion of *Cryptococcus neoformans*

Carolina Coelho[*,†], **Ana Camila Oliveira Souza**[‡], **Lorena da Silveira Derengowski**[‡], **Carlos de Leon-Rodriguez**[*], **Bo Wang**[*,§], **Rosiris Leon-Rivera**[¶], **Anamelia Lorenzetti Bocca**[‡], **Teresa Gonçalves**[†], and **Arturo Casadevall**[*]

[*]Department of Microbiology and Immunology, Albert Einstein College of Medicine of Yeshiva University, Bronx NY 10461

[†]Centre for Neuroscience and Cell Biology, University of Coimbra and Faculty of Medicine, University of Coimbra, 3004-504 Coimbra, Portugal

[‡]Cell Biology Department, Biology Science Institute, University of Brasilia, Brazil

[§]MD Program, Albert Einstein College of Medicine of Yeshiva University, Bronx NY 10461

[¶]Department of Biology, University of Puerto Rico, Río Piedras Campus, San Juan, PR and Undergraduate Research Program, Albert Einstein College of Medicine of Yeshiva University, Bronx NY 10461

Abstract

Human infection with *Cryptococcus neoformans* (Cn), a common fungal pathogen follows deposition of yeast spores in the lung alveoli. The subsequent host-pathogen interaction can result in either eradication, latency or extra-pulmonary dissemination. Successful control of Cn infection is dependent on host macrophages but macrophages display little ability to kill Cn *in vitro*. Recently, we reported that ingestion of Cn by mouse macrophages induces early cell cycle progression followed by mitotic arrest, an event that almost certainly reflects host cell damage. The goal of the present work was to understand macrophage pathways affected by Cn toxicity. Infection of macrophages by Cn was associated with alterations in protein translation rate and activation of several stress pathways such as Hypoxia Inducing Factor-1α (HIF-1α), Receptor-interacting Protein 1 (RIP1) and Apoptosis Inducing Factor (AIF). Concomitantly we observed mitochondrial depolarization in infected macrophages, an observation that was replicated *in vivo*. We also observed differences in the stress pathways activated depending on macrophage cell type, consistent with the non-specific nature of Cn virulence known to infect phylogenetically distant hosts. Our results indicate that Cn infection impairs multiple host cellular functions and undermines the health of these critical phagocytic cells, which can potentially interfere with their ability to clear this fungal pathogen.

Address correspondence and reprint requests to Arturo Casadevall, Forchheimer 411, 1300 Morris Park Avenue, Bronx, NY 10461. Telephone: +1718-430-3766 Fax: +1718-430-8711. arturo.casadevall@einstein.yu.edu.

Introduction

The interaction of the pathogenic fungus *Cryptococcus neoformans* (Cn) with macrophages is thought to be a critical event in the course of cryptococcal infection (1–8). However host macrophages show little fungicidal activity in vitro (7, 9) and instead allow Cn to reside in a mature acidic phagolysosome where it replicates. Cn is believed to use macrophages for extrapulmonary dissemination in a Trojan horse strategy (10). Moreover, the ability for replication within the phagosome is correlated with increased virulence (1, 11, 12) originating the notion that Cn is a facultative intracellular pathogen.

Survival of Cn in the phagolysosome has been attributed to various fungal characteristics (13, 14) of which the most prominent is a large polysaccharide capsule but many others are essential for infection such as melanin and phospholipase B1. Although ingestion of Cn by macrophages is followed by many hours where the host cell is viable, several studies have reported damage to host cellular processes including: increased phagosome permeability (1), inhibition of cyclin D1 (15) and DNA instability (16), followed by mitotic arrest (17). Furthermore intracellular residence of Cn decreases antigen presentation, T cell proliferation and cytokine production by macrophages (18, 19). Additional evidence of host cell damage is apparent when large residual vacuoles are observed in macrophages from which Cn has exited by non-lytic exocytosis (20). However, the mechanisms by which Cn damages cells have not been investigated in detail.

Intracellular pathogens have evolved strategies to manipulate host machinery for their survival (21). Interference with signal transducer activity, manipulation of the lysosomal compartment and host cell survival vs death are a few examples of commonly targeted processes. For example both *Francisella* and *Mycobacterium* possess virulence factors that decrease caspase-1 activation and therefore decreasing production of caspase-1 derived inflammatory IL-1β (22). Cell death pathways rely on mitochondrial mediators for, at least, a portion of the pathway, and therefore many survival vs death decisions are integrated in the mitochondria. Additionally mitochondria are no longer regarded solely as the cell's powerhouse but also play a role in immune function, producing Reactive Oxygen Species (ROS) (23) for activation of the inflammasome (24). Consequently viral, bacterial and protozoan pathogens have a myriad of factors that manipulate host cell mitochondria (25, 26) but comparable information is not yet available for fungal pathogens.

Current views of Cn intracellular pathogenesis posit a passive resistance of fungi to host attack while little has been done to explore active fungal attack on the host. Survival of the host cell after non-lytic exocytosis and the absence of widespread host cell death in Cn-macrophage studies has encouraged the view that host cells suffer little or no damage from this organism. In this work, we have investigated macrophage injury after Cn infection. Our results indicate Cn phagocytosis results in modifications of critical cellular functions including impaired mitochondrial function, activation of caspase-1 and cellular stress pathways and altered protein synthesis rate. The accumulation of cellular damage associated with Cn intracellular residence could promote and potentiate Cn survival in macrophages and contribute to cryptococcal virulence.

Materials and Methods

Fungal strains

C. neoformans var. *grubii* strain H99 (serotype A), acapsular mutant cap59 and original wild-type K99 were a kind gift of Joseph Heitman (Durham, NC). Yeast cells for infection were grown for 2 d in Sabouraud dextrose broth (Difco, Carlsbad, California) at 37°C.

Macrophage and macrophage-like cells

Three types of macrophages were used for most experiments: the macrophage-like murine cell line J774.16 (27), Bone Marrow Derived Macrophages (BMDM) and peritoneal macrophages. J774.16 were kept in DMEM complete media consisting of DMEM (CellGro), 10% NCTC-109 Gibco medium (LifeTechnologies), 10% heat-inactivated FBS (Atlanta Biologicals), and 1% non-essential amino acids (CellGro). BMDM were obtained by extracting bone marrow from hind leg bones of 6–8 weeks BALB/C female mice (National Cancer Institute) and maturing them in vitro for 6–8 d in DMEM media with 20% L-929 cell conditioned media, 10% fetal bovine serum, 2 mM L-glutamine (CellGro), 1% non-essential amino acids (CellGro), 1% HEPES buffer (CellGro) and β-mercaptoethanol (Gibco). Peritoneal macrophages were extracted by injecting 10 mL of ice-cold PBS into mice peritoneal cavity, cultured and infected in the same conditions as J774.16 cells. Peritoneal macrophage population was defined as adherent CD11b + cells. In all assays macrophages were plated to achieve a density of 1×10^5 cells /mL at time of Cn infection. Cn were added at a Multiplicity of Infection (MOI) of 1:2 (unless otherwise noted) along with capsular monoclonal antibody (mAb) 18B7 (28) at 10 μg/mL. For some experiments Cn was killed with heat (HK Cn) by incubation at 60°C for 60 min or with oxidative damage by incubating yeast pellet with 30% (w/w) H_2O_2 for 30 min. All animal experiments were conducted according to ethical guidelines, with the approval of the Institutional Animal Care and Use Committee of Albert Einstein College of Medicine.

Killing and caspase activation assays

For fungal killing assays the cells were detached by vigorous pipetting and diluted in sterile water onto Saboraud agar plates. Colony Forming Units (CFU) were counted after 2 d at 30°C. Specific caspase activity was detected using a Fluorochrome Inhibitor of Caspases (FLICA) (Immunochemistry Technologies) assay. Briefly carboxyfluorescein-labeled inhibitor peptide was added 1 h before the termination of phagocytosis and stained with 0.1 μg/mL of Hoechst for detection of necrotic/late apoptotic cells. Cells were analyzed immediately by Laser Scanning Cytometry in the iCys® Research Imaging Cytometer (CompuCyte Corporation) (17). Caspase activation was measured by imaging 20–40 fields in each well with the 40× objective at 0.5 μm resolution, allowing a field size of 500 μm×192 μm.

ATP, LDH and glucose measurements

Total ATP content and Lactate dehydrogenase (LDH) release can be used to estimate cell numbers and cellular viability. ATP measurements were performed by adding Triton-X100 at 0.25% and 2 mM EDTA (Sigma-Aldrich) to the wells containing infected cells. Next, 25

µl of this extract was incubated with Enliten ATP assay system (Promega) and counts per second (CPS) measured in a standard luminometer. We confirmed in each assay extraction of ATP solely from mammalian cells and no extraction of Cn-derived ATP, as indicated by the manufacturer. LDH and glucose were measured by enzymatic reactions (Abcam), following manufacturer's instructions. Briefly, for LDH 10 µL of macrophage supernatants were added to 100 µl of enzymatic mix and absorbance was read after 30 min at 450 nm. For glucose 1:100 dilutions of cell supernatants were mixed with assay mix and glucose content determined by comparison with glucose standards.

Immunoblot analysis

Cytosolic protein extracts were obtained by re-suspending the cell pellet in 250 mM sucrose, 50 mM Tris-HCl pH 7.4, 5 mM $MgCl_2$ and total cell extracts were obtained in RIPA buffer. Both were supplemented with cOmplete Mini Protease Inhibitor Cocktail (Roche Applied Science), followed by 20 strokes with a Dounce homogenizer and centrifugation at 3000 rpm for 10 min for cytosolic extracts or 14000 rpm for 30 min for total cell extracts. Western blot was performed in a NuPAGE SDS-PAGE (LifeTechnologies) system for the following primary antibodies: rabbit anti-AIF and mouse anti-RIP (1:2000 to 1:200, from BD Biosciences), cleaved PARP D-214 (Cell Signaling), mouse anti-cytochrome c (1:200) (clone 7H8.2C12, Abcam) and MFN1 (H-65) and MFN2 (H-68, Sta. Cruz Technologies). β-actin antibody coupled to peroxidase (1:5000, Sta. Cruz Technologies) was used as a loading control.

Gene expression

Macrophages were plated to achieve a density of 8×10^6 cells at the time of infection on 10 cm^2 dishes and infected as before. RNA was extracted using a RNeasy Mini Kit (Qiagen) and stored at −80C until analysis. Gene expression analysis was performed at Genome Technology Access Center in the Department of Genetics at Washington University School of Medicine. Briefly, a total of 10 µg of RNA was converted to cDNA using the Nugen Pico SL (Nugen) and labelled using Nugen Encore Biotin kit. Target cRNA was hybridized to the murine genome Affymetrix Mouse Gene 1.0 st (Affymetrix). Biological replicates were performed 4 times and each experimental set analyzed separately and then averaged for data analysis. All microarray datasets (CEL files) were normalized with ExonRMA algorithm. Data variance was stabilized, transformed on logarithmic scale and quality control was performed. Genes were considered differentially expressed if p-value < 0.05 and fold change above 1.5. Genes satisfying these conditions were imputed into Ingenuity Pathway Analysis (Ingenuity® Systems, www.ingenuity.com) for analysis of upstream regulators and Gene Ontology. Gene expression analysis was confirmed by RT-qPCR for selected genes (list of primers in Supplemental Table 1).

Ribopuromycylation (RPM) and immunofluorescence

Cells were infected as described above and 15 min before the end of the experiment media was supplemented with 91 µM puromycin and 208 µM emetine. One well was left without puromycin and used as negative control (C−). Cells fixed with 3% paraformaldehyde, protease inhibitors cocktail cOmplete Mini (Roche), 0.015% digitonin and 10 U /mL of RNaseOUT in 50mM Tris-HCl buffer for 15 min at room temperature, blocked in a solution

of 0.05% saponin, 1 μg/mL of Fc block antibody (BD Biosciences), 10 mM glycine and 5% FBS in PBS for 10 min, followed by addition of 1:100 of 2D10-conjugated to Alexa 488 or Alexa 647 fluorophores, a kind gift of Jonathan W Yewdell (NIAID). Cells were counterstained with Hoechst at 0.1μg/mL and fluorescence quantified in iCys Compucyte LSC. For mitochondrial morphology cells were plated in optical quality dishes (Maktek Corporation), stained for RPM as before or with Alexa 488 conjugated-cytochrome c antibody, clone 6H2.B4 (BDPharmingen) and imaged 0.2 μm steps with Inverted Olympus IX71 coupled to a Photometrics CoolSnap HQ CCD camera and analyzed using Volocity 3D (Perkin Elmer).

Mitochondrial potential (Δφm) and Reactive Oxygen Species (ROS) measurements

Jc-1 was added 15 min before termination of assay, according to manufacturer instructions (Immunochemistry Technologies). Jc-1 dye accumulates as a red aggregate in healthy mitochondria and as a green monomer in depolarized mitochondria. ROS were measured with CellROX® Deep Red Reagent (LifeTechnologies) for 30 min at 5 μM concentration. TMRE and Mitotracker green were added to the cells for 45 min before termination of the experiment at 200 and 25 nM, respectively. For *in vivo* experiments mice were infected with 1×10^7 Cn i.p. or sterile PBS (vehicle) for the indicated time and 30 min before sacrifice each mouse received 30 μL of Jc-1 dye diluted in PBS was also injected i.p. Peritoneal lavage cells were immunostained with CD45-PercP-Cy5.5 (eBiosciences) and F4/80-Alexa 647 (Life Technologies) and Uvitex for exclusion of extracellular yeasts. Fluorescent signal from viable cells, as measured by DAPI exclusion, was detected in a Becton Dickinson LSRII instrument (BD Biosciences).

Transmission Electron Microscopy (TEM)

Macrophages were infected with Cn for 24 h and fixed with 2% glutaraldehyde, 4% paraformaldehyde in 0.1 M cacodylate at room temperature for 2 h, followed by overnight incubation in 4% formaldehyde, 1% glutaraldehyde in PBS. The samples were subjected to postfixation for 90 min in 2% osmium, serially dehydrated in ethanol, and embedded in Spurrs epoxy resin. Sections (70–80 nm thick) were cut on a Reichart Ultracut UCT and stained with 0.5% uranyl acetate and 0.5% lead citrate. Samples were viewed in a JEOL 1200EX transmission electron microscope at 80 kV.

Statistical analysis and plotting

Graphs, statistical analysis and figures were assembled in Prism version 6.00 for Mac OS X, GraphPad Software, San Diego, California, USA. Figure 4 was generated using String database (29).

Results

Gene expression changes upon infection of J774.16 macrophage-like cells following opsonic ingestion of Cn

We investigated gene expression changes occurring in J774.16 macrophage-like cell line at 2 and 24 h after ingestion of yeast cells (Fig. 1 and full gene list in Supplemental Table 2). Initial gene expression changes could be observed already at 2 h post-infection, with much

larger changes becoming apparent at 24 h of infection. Ingestion of live Cn by macrophages differentially modulated the expression of 110 genes while infection with HK Cn affected 61 genes. There were very few genes differentially modulated by both live and dead yeast cells: *Srrt* was down-regulated at 24 h and *Ccl2, Ccl7, Gas5, Glipr1, Gprc5a, Hmgb1, Phlda1, Id2, Sh3pxd2a, Mup2, Rhob* and *Snhg1* levels were altered after 2 h. When macrophages were infected with live Cn there were 3 genes that remained up-regulated throughout the course of infection: *Emp1, Serpine1* and *Id2* (confirmed by RT-PCR in Supplemental Fig. 1). Ingenuity Pathway Analysis of gene expression changes showed that after 2 h of infection the macrophages upregulated pathways involved in cell death and survival, cellular movement, proliferation and cell-to-cell signaling. Predicted Upstream Regulators activated at this time are Platelet-Derived Growth Factor BB (PDGFBB), Receptor activator of nuclear factor kappa-B ligand (TNFS11 or RANKL) and Triggering Receptor Expressed on Myeloid Cells (TREM1). PDGFBB is a mitogenic factor, TNFS11 is an anti-apoptotic cell survival factor (30) and TREM1 was recently described as a hypoxia responsive factor (31) that is involved in the response to *Aspergillus fumigatus* (32). Analysis of genes affected at 24 h revealed activation of such cellular functions as amino acid metabolism, post-translational modifications, small molecule biochemistry, cell growth and proliferation and cell death and survival. Predicted upstream regulators activated at 24 h were IL-4, IL-5, Hypoxia-Inducible Factor-1-α (HIF1-α) and CD38. Both IL-4 and IL-5 are Th2 associated cytokines and both have been found in cryptococcal infected mouse lungs (33). HIF1-α is a major regulator of response to hypoxia that was associated with fungal pathogenesis (34). CD38 is an enzyme responsible for the synthesis and hydrolysis of cyclic ADP-ribose from NAD+ and loss of this enzyme impairs immune responses to *Listeria monocytogenes* (35). In summary, gene expression changes in J774.16 cells upon Cn infection were consistent with those reported *in vivo* and indicated simultaneous activation of immune and stress responses.

Cn infection of murine macrophages alters protein translation rate in host cells

To further explore possible mechanisms that could eventually lead to Cn-induced cell stress, we investigated protein synthesis, activation of cellular death pathways and mitochondrial function in Cn infected macrophages. Consequently we measured macrophage protein synthesis rate by using immunofluorescence to detect puromycin binding to nascent mRNA chains (36). Quantification of ribosome bound puromycin revealed a decrease in the rate of translation in J774.16 macrophage-like cell line infected with Cn (Fig. 2A). This observation agrees with the gene expression data suggesting a modulation of post-translational modifications. However when we replicated the experiments in primary macrophages extracted from the peritoneal cavity we observed an increase in rate of translation upon Cn infection (Fig. 2B). None of the cells showed alterations in the cellular distribution of the active ribosomes as seen by fluorescence microscopy (Fig. 2C). Thus, while Cn-infection can modulate overall rate of protein synthesis in macrophages, we did not observe a uniform pattern of increased or decreased protein synthesis in the infected macrophage subsets.

Cn infection of murine macrophages and J774.16 macrophage-like cell line results in major changes in macrophage metabolism and only partial restriction of Cn growth *in vitro*

Cn infection of murine macrophages results in restriction of fungal growth and some degree of fungal killing for the first 24 h of infection (Fig. 3A). Live cell microscopy has shown that during the first 24 h of infection Cn and macrophage cells coexist *in vitro* with over 90% of macrophages remaining viable (unpublished data). We found that commonly used methods to measure cell viability by colorimetry (tetrazolium dye reduction and nuclear dye incorporation) were unreliable because we could not separate yeast and macrophage contributions to measurements. Consequently, we used total ATP levels as a measure of macrophage number based on selective extraction of ATP from macrophages and not from yeast cells. With this approach we confirmed that ATP levels in infected cells decreases to 80–60% when compared to uninfected cells in the first 24 h (Fig. 3B), indicating that Cn infection is accompanied by either severe biochemical changes in the surviving cells, a small degree of macrophage cell death, or both of these processes.

Cn infection can activate Programmed Cell Death Pathways in murine macrophages and macrophage-like J774.16 cells

To further explore whether Cn-induced intracellular stress could result in accelerated macrophage death, we assessed activation of Programmed Cell Death effector molecules, such as caspases, Apoptosis Inducing Factor (AIF) and Receptor-Interacting Kinase 1 (RIP). The J774.16 macrophage-like cell line showed a trend to activate caspase-1 and caspase-3 throughout infection, but this result did not reach statistical significance (Fig. 4), while BMDM activated caspase-1,-3 and -8. Furthermore, we determined that killing of yeast cells by J774.16 or BMDM macrophages *in vitro* was not affected by pan-caspase inhibition but was decreased by inhibition of NO formation (Supplemental Figure 2). When we assessed protein expression of apoptosis pathway intermediates, J774.16 macrophage-like cells increased expression of RIP and AIF early in the course of infection (Fig. 4B–C) while BMDM showed activation of AIF and released cytochrome c into the cytosol. Furthermore, there was an increase of J774.16 cells with Annexin V externalization as well as cells with both Annexin V externalization and Propidium Iodide (PI) permeability (Fig. 4D). Additionally, J774.16 cells increased LDH levels in supernatants (Fig. 4E), providing a clue that Cn infection in J774.16 cells caused a type of necrotic death. No detectable LDH release was found in BMDM (data not shown) which together with the activation of caspase-3 indicates classical features of apoptosis in BMDM. In addition, we measured glucose concentration in supernatants and found no difference of infected macrophages relative to non infected cells, ruling out glucose depletion due to fungal growth as a mechanism for macrophage toxicity (Fig. 4F). We then proceeded to test primary peritoneal macrophages, observing that peritoneal macrophages activated caspase-3 and increased their LDH levels in the supernatant. Results are summarized in Table 1. Thus, while only a small subset of macrophages died upon the first 24 h of Cn infection, we showed that Cn induced cellular stress pathways and necrotic and apoptotic features in a variety of infected macrophages; however, we also observe that the type of stress and death pathway activated was dependent on macrophage type.

Murine macrophages and J774.16 macrophage-like cells depolarize mitochondria after infection with Cn

Given that mitochondria are critical for many aspects of cellular homeostasis we studied mitochondrial potential (Δϕm) alterations (37). Mitochondrial potential can be measured through incorporation of fluorescent dyes where brightness of tetramethylrhodamine (TMRE) is proportional to Δϕm. For the dye 5,5′,6,6’-tetrachloro-1,1’,3,3′-tetraethylbenzimidazolylcarbocyanine iodide (Jc-1) the color of cells will shift from green to red as mitochondrial hyperpolarize. Therefore the ratio of red/green will allow for semiquantitative measurement of Δϕm (37). As experimental controls we added carbonyl cyanide m-chlorophenyl hydrazone (CCCP-1) to depolarize mitochondria or rotenone (Rot) to hyperpolarize mitochondria. All macrophage depolarized their mitochondria at 24 h of infection (Fig. 5A–C). We note that for BMDM Δϕm was decreased to a much lower extent than for the other cell types (Fig. 5B), and because this cell type was also resistant to CCCP-1 depolarization we suggest the existence of a cell-type specific resistance to depolarization. Transmission Electron Microscopy revealed no alterations in mitochondrial ultrastructure (Fig. 5D) but depolarization of mitochondria was accompanied by alterations in the mitochondrial network with increased fission in infected cells (Fig. 5E). This suggests that mitochondria are not directly damaged by infection, but rather have their activity modulated by prolonged Cn residence. Our attempts to modulate Δϕm in macrophages were unsuccessful because mitochondrial inhibitory drugs were highly toxic to Cn cells (data not shown). We investigated if *Acanthamoeba castellanii* could modulate their mitochondria upon ingestion of Cn but found no difference in Δϕm in these unicellular organisms (data not shown).

Mitochondrial alterations do not correlate with oxidative burst but are mediated by NO

We evaluated whether mitochondrial modulation was related to ROS (24) and NO levels (38). We found that neither J774.16 nor BMDM produced significant amounts of ROS after phagocytosis of Cn (Fig. 6A, data not shown for BMDM). To discard the possibility that the observed lack of ROS production was due to a quenching effect of Cn we exposed macrophage cells to zymosan, a preparation of *Saccharomyces cerevisiae* cell wall, and H_2O_2-killed Cn, but none of these conditions triggered ROS production in J774.16 macrophage-like cells (Fig. 6B). Peritoneal macrophages were capable of releasing ROS in response to Cn (data not shown) and when exposed to zymosan or H_2O_2-killed (Fig.6C). However ROS production by mitochondria occurs upon mitochondrial hyperpolarization and therefore in the particular case of Cn infection in peritoneal macrophages it is likely that Δϕm modulation is disconnected from ROS production. When S-ethyl-iso-thiourea (SEITU), an inhibitor of NO, was added to H99 infected J774.16 macrophage-like cells and to peritoneal macrophages (data not shown) depolarization was decreased at 24 h of infection (Fig. 6D), suggesting a role for NO in mitochondrial depolarization.

Intraperitoneal infection of mice with Cn causes a decrease in mitochondrial polarization in peritoneal total leukocytes and macrophages

We proceeded to investigate if the mitochondrial depolarization observed *in vitro* was also observed *in vivo.* In a model of peritoneal Cn infection we observed that peritoneal lavage

cells, both total leukocytes (CD45+) and macrophages (F4/80+) were depolarized at 24 h post-infection in comparison with mock infected mice (Figure 7), validating our *in vitro* findings in a murine model of infection. Overall our results show multiple alterations in macrophage functions upon Cn infection, namely gene expression changes, alterations of protein translation rates and alteration in mitochondrial dynamics (summarized in Table 1).

Discussion

There is now considerable evidence that intracellular residence of Cn is associated with damage to macrophages, as evidenced by phagosomal leakiness (1), giant vacuole formation (20) and cell cycle arrest (17). Since progressive accumulation of cellular damage can result in cell death we set out to investigate the mechanisms of macrophage cell damage after Cn phagocytosis with a specific focus on mitochondrial function, a major integrator of cellular decisions such as survival, oxidative burst and immune responses (24). Our initial studies focused on determining whether host cell gene expression changes that could potentially explain the results previously reported. The transcript level of dozen of genes was affected, many of those genes related to a stress response, and these changes were consistent with phenotypic observations following Cn infection of macrophages. For example previous work has shown that initial proliferation of macrophages infected with Cn is followed by cell cycle arrest (17, 39). Gene expression data here provides information consistent with and supportive of the cell cycle changes observed. PDGFBB, which belongs to the same family as CSFR1 and is a mitogenic factor for endothelial cells (40), could be a mediator of the initial proliferation, while activation of HIF1-α (41) and cyclin G2 (42) at later times might contribute to cyclin D1 inhibition (15) and the subsequent cell cycle arrest upon Cn infection (17). The protein synthesis machinery is a target for viral (43), bacterial and parasitic pathogens (44, 45). Translation interference by fungal pathogens was suggested for *Candida albicans* and in Cn infection (discussed in (45)), but had not been shown for fungal infections thus far.

Next we demonstrated that Cn intracellular residency affected cell stress, survival and death responses. We observed a low mortality of infected macrophages and no pathway predominated to trigger wholesale cell death, as determined by the mixed pattern of activation of death pathways. It is possible that simultaneous interferences in multiple pathways, despite being small in magnitude, could result in significant effects in macrophage health and ability to clear the pathogen when combined. Cn resides and replicates within host macrophages but the host cells do not typically display features of necrotic or apoptotic deaths. Interestingly, Th1 activation of macrophages decreases the amount of lysosomal damage to the host cells and therefore macrophage damage can be modulated by the cytokine milieu (Davis et al., joint submission), providing further evidence that equilibrium between host and pathogen is modulated by the cytokine milieu (33, 46). The absence of a predominant death pathway, combined with inability of macrophages to eliminate Cn, phagosomal leakiness and cell cycle arrest may be caused by multiple subtle alterations in cellular function, including mitochondrial function. Our results are consistent with capacity of Cn to causes latent infection in granulomas, with long-term survival of both host and pathogen (3, 8), while concomitantly Cn residency in macrophages causes enough dysfunction that could explain the suboptimal stimulation of immune responses reported

previously (18, 19). Finally, our data are consistent with the scenario that macrophage death is likely to occur in a small subset of cells, in which the cumulative damage induced by Cn exceeds certain threshold, and depending on the type of cellular response this cell death can become either apoptotic or necrotic.

Cn infection caused a decrease in $\Delta\phi m$ in all macrophage cell types tested, an observation previously reported for bacterial pathogens *Shigella flexneri* (47) and *Mycobacterium tuberculosis* (48). Mitochondrial depolarization occurred in every macrophage type tested and in a mouse model of infection, suggesting that this is a conserved response to Cn infection. The necessity for mitochondrial modulation derives both from regulation of fuel and energy requirements and from the emerging role of mitochondria as integrators of cellular decisions of death, survival and immune activation (24). For example, mitochondrial depolarization reflects a metabolic switch essential for T lymphocyte (49) and dendritic cell activation, allowing immune cells to survive in hypoxic environments and undergo rapid proliferation (38). Similarly, mitochondrial signaling is necessary for macrophage activation and might even contribute directly to microbicidal abilities (23). In our model such a metabolic switch *in vitro* could be triggered by either TREM1 (50), HIF-1α or CD38 (51, 52), as suggested by the gene expression data, since each of them can regulate mitochondrial activity and metabolism. It was suggested that a possible role of mitochondria is to produce ROS for activation of the inflammasome (24); however, our data does not support a role for mitochondrial ROS in Cn infection. Instead our data suggests a role for NO in mitochondrial modulation (38, 53) where prolonged inhibition of NO attenuates mitochondrial depolarization. An added complexity to the mitochondrial equation is that Cn requires both the glycolytic pathway and the mitochondria for full virulence (54, 55) and therefore mitochondrial functions are crucial for both sides of host pathogen interaction (56).

Macrophage heterogeneity based on different anatomical sources (57) or culture conditions (58) is well established, a fact that has been attributed to adaptations to their local microenvironment. Given this heterogeneity we evaluated three macrophage types for their interaction with Cn, and observed that each responded differently. Our study did not investigate alveolar macrophages due to concerns about the relevance of this cell in host defense. Although alveolar macrophages are presumably the first to come contact with Cn their role in host defense in mice is unclear since their depletion reduces vulnerability to infection (7). In fact, alveolar macrophages are in a minority in the infected lungs, as they become rapidly outnumbered by bone-marrow (monocyte) derived exudate macrophages during the inflammatory response to infection. Consequently, exudate macrophages are the major subset of mononuclear effector cells in the lungs (59), and therefore our studies focused on macrophage types that resemble exudate macrophages. Finally, one must consider that virulence is a complex equation (60) and acknowledge that one limitation of this work is that we studied only one Cn strain and that there may strain specific factors that could produce strain dependent outcomes in Cn-macrophage interactions (12). Given these observed heterogeneity in responses of host to pathogen we propose two scenarios to explain these results. Toxicity might have started with disruption of one cellular process that then cascaded to affect multiple cell processes. For example mitochondrial alterations can potentiate ER stress (61) or alternatively mitochondrial alterations could be caused by

deregulation of cyclin D1 (62). In any case our data provides multiple explanations for the previously reported cell cycle arrest upon Cn ingestion (17). According to this view the differences observed in activation of programmed cell death pathways would reflect a heterogeneous response to Cn inflicted stress due to cell type anatomic origin and the differences between J774.16 and the other macrophages could reflect differences between an immortalized cell line and primary cells. Alternatively one might hypothesize that Cn causes damage to various cellular systems, which in turn results in multiple hits to the host cell. The absence of a specific damage pathway is intriguing until one considers that Cn can infect a great variety of hosts including mammals, worms, insects, plants and amoebae, and that its virulence for mammals may be accidental (63). In this regard Cn is very different from pathogenic microbes with narrow host ranges, such as certain viruses that depend on one host, which have evolved precise mechanisms to manipulate host biology and immune responses. In contrast, our results show that Cn inflicts damage to cell by multiple mechanisms and, when this distinction is considered, such a cell pathogenic strategy can be understood in the sense that it allows survival in many different cell types. The fact that in contrast to macrophages Cn-infected amoebae did not manifest mitochondrial depolarization is consistent with this view, which posits different damage to different hosts. These scenarios are not mutually exclusive.

In summary, our results establish that macrophages activate several immune defense mechanisms upon Cn infection but are unable to effectively clear fungal infection *in vitro*. Residency of fungal cells in macrophages was associated with a progressive deterioration in host cellular functions. Specifically Cn ingestion activated several stress pathways, affected protein translation and caused mitochondrial depolarization. Our results provide evidence for subtle cytopathic effects of Cn on macrophages, that with time could progress to eventual cell death, as evident by the small percentage of macrophage death at 24 h. This damage could help the persistence of Cn within macrophages, inability to clear Cn infection and inefficient immune responses translating into chronic infections. We established that mitochondrial modulation is a significant factor in fungal infection of macrophages, as shown for bacterial infections (38, 64). The multiple hit intracellular survival strategy, illustrated here, provides a paradigm for understanding how pathogens, such as Cn, are able to infect such evolutionarily distant hosts, ranging from Kingdom Protozoa to Animalia.

Supplementary Material

Refer to Web version on PubMed Central for supplementary material.

Acknowledgments

Acknowledgments and Conflict of Interest:

This work was supported by NIH awards 5R01HL059842, 5R01AI033774, 5R37AI033142, and 5R01AI052733 (to A.C.), and Center for AIDS Research at Einstein. CC was a recipient of a PhD grant by Fundação Ciência e Tecnologia (SFRH / BD / 33471 / 2008) under the PhD Program in Experimental Biology and Biomedicine of the CNC, University of Coimbra, Portugal and PEst-C/SAU/LA0001/2013-2014. Rosiris Leon Rivera was supported through a Minority Access to Research Careers (MARC) program 5T34GM007821-31.

Genomic data experiments were performed at the Genome Technology Access Center in the Department of Genetics at Washington University School of Medicine, partially supported by NCI Cancer Center Support Grant

#P30 CA91842 to the Siteman Cancer Center and by ICTS/CTSA Grant# UL1RR024992 from the National Center for Research Resources (NCRR), a component of the National Institutes of Health (NIH), and NIH Roadmap for Medical Research. Analytical Imaging Facility of Albert Einstein College of Medicine is supported through NCI cancer center support grant P30CA013330. Computational Genomics Facility of Albert Einstein College of Medicine helped with statistical analysis and data was deposited as GSE57720 (http://www.ncbi.nlm.nih.gov/geo/query/acc.cgi?acc=GSE57720).

(The data in this paper are from a thesis submitted by Carolina Coelho in partial fulfillment of the requirements for the degree of Doctor of Philosophy in the Faculty of Medicine, University of Coimbra, 3004-504 Coimbra, Portugal).

The authors wish to thank Juliana Rizzo for help with amoeba experiments not included in the final version of the manuscript and Dr. Jonathan W Yewdell for help with ribopuromycylation experiments.

We would like to acknowledge all the personnel at Analytical Imaging Facility, in particular Vera DesMarais, Hillary Guzik, Ben Clark and Geoffrey Perumal for their technical assistance. We would like to thank Computational Genomic facility, Dept. of Genetics, Albert Einstein College of Medicine for help with data analysis.

References

1. Tucker SC, Casadevall A. Replication of Cryptococcus neoformans in macrophages is accompanied by phagosomal permeabilization and accumulation of vesicles containing polysaccharide in the cytoplasm. Proceedings of the National Academy of Sciences of the United States of America. 2002; 99:3165–3170. [PubMed: 11880650]
2. Osterholzer JJ, Milam JE, Chen GH, Toews GB, Huffnagle GB, Olszewski MA. Role of Dendritic Cells and Alveolar Macrophages in Regulating Early Host Defense against Pulmonary Infection with Cryptococcus neoformans. Infect. Immun. 2009; 77:3749–3758. [PubMed: 19564388]
3. Feldmesser M, Kress Y, Novikoff P, Casadevall A. Cryptococcus neoformans is a facultative intracellular pathogen in murine pulmonary infection. Infect. Immun. 2000; 68:4225–4237. [PubMed: 10858240]
4. Qin QM, Luo J, Lin X, Pei J, Li L, Ficht TA, de Figueiredo P. Functional analysis of host factors that mediate the intracellular lifestyle of Cryptococcus neoformans. PLoS pathogens. 2011; 7:e1002078. [PubMed: 21698225]
5. Gordon S. Alternative activation of macrophages. Nat Rev Immunol. 2003; 3:23–35. [PubMed: 12511873]
6. Brown GD. Innate Antifungal Immunity: The Key Role of Phagocytes. Annu. Rev. Immunol. 2011:1–21. [PubMed: 20936972]
7. Shao X, Mednick A, Alvarez M, Van Rooijen N, Casadevall A, Goldman DL. An Innate Immune System Cell Is a Major Determinant of Species-Related Susceptibility Differences to Fungal Pneumonia. The Journal of Immunology. 2005; 175:3244–3251. [PubMed: 16116215]
8. Goldman DL, Lee SC, Mednick AJ, Montella L, Casadevall A. Persistent Cryptococcus neoformans pulmonary infection in the rat is associated with intracellular parasitism, decreased inducible nitric oxide synthase expression, and altered antibody responsiveness to cryptococcal polysaccharide. Infect. Immun. 2000; 68:832–838. [PubMed: 10639453]
9. Vecchiarelli A, Pietrella D, Dottorini M, Monari C, Retini C, Todisco T, Bistoni F. Encapsulation of Cryptococcus neoformans regulates fungicidal activity and the antigen presentation process in human alveolar macrophages. Clinical and experimental immunology. 1994; 98:217–223. [PubMed: 7955525]
10. Kechichian TB, Shea J, Del Poeta M. Depletion of alveolar macrophages decreases the dissemination of a glucosylceramide-deficient mutant of Cryptococcus neoformans in immunodeficient mice. Infect. Immun. 2007; 75:4792–4798. [PubMed: 17664261]
11. Levitz SM, Nong SH, Seetoo KF, Harrison TS, Speizer RA, Simons ER. Cryptococcus neoformans resides in an acidic phagolysosome of human macrophages. Infect. Immun. 1999; 67:885–890. [PubMed: 9916104]

12. Alanio A, Desnos-Ollivier M, Dromer F. Dynamics of Cryptococcus neoformans-macrophage interactions reveal that fungal background influences outcome during cryptococcal meningoencephalitis in humans. MBio. 2011:2.
13. Coelho C, Bocca AL, Casadevall A. The Tools for Virulence of Cryptococcus neoformans. Adv. Appl. Microbiol. 2014; 87:1–41. [PubMed: 24581388]
14. Vecchiarelli A, Pericolini E, Gabrielli E, Kenno S, Perito S, Cenci E, Monari C. Elucidating the immunological function of the Cryptococcus neoformans capsule. Future Microbiol. 2013; 8:1107–1116. [PubMed: 24020739]
15. Luo Y, Casadevall A. Intracellular cryptococci suppress Fc-mediated cyclin D1 elevation. Commun Integr Biol. 2010; 3:390–391. [PubMed: 20798836]
16. Ben-Abdallah M, Sturny-Leclere A, Ave P, Louise A, Moyrand F, Weih F, Janbon G, Memet S. Fungal-induced cell cycle impairment, chromosome instability and apoptosis via differential activation of NF-kappaB. PLoS pathogens. 2012; 8:e1002555. [PubMed: 22396644]
17. Coelho C, Tesfa L, Zhang J, Rivera J, Gonçalves T, Casadevall A. Analysis of cell cycle and replication of mouse macrophages after in vivo and in vitro Cryptococcus neoformans infection using laser scanning cytometry. Infect. Immun. 2012; 80:1467–1478. [PubMed: 22252872]
18. Vecchiarelli A, Dottorini M, Pietrella D, Monari C, Retini C, Todisco T, Bistoni F. Role of human alveolar macrophages as antigen-presenting cells in Cryptococcus neoformans infection. Am J Respir Cell Mol Biol. 1994; 11:130–137. [PubMed: 8049074]
19. Retini C, Vecchiarelli A, Monari C, Bistoni F, Kozel TR. Encapsulation of Cryptococcus neoformans with glucuronoxylomannan inhibits the antigen-presenting capacity of monocytes. Infect. Immun. 1998; 66:664–669. [PubMed: 9453624]
20. Alvarez M, Casadevall A. Cell-to-cell spread and massive vacuole formation after Cryptococcus neoformans infection of murine macrophages. BMC Immunol. 2007; 8:16. [PubMed: 17705844]
21. Thi EP, Lambertz U, Reiner NE. Sleeping with the enemy: how intracellular pathogens cope with a macrophage lifestyle. PLoS pathogens. 2012; 8:e1002551. [PubMed: 22457616]
22. Bergsbaken T, Fink SL, Cookson BT. Pyroptosis: host cell death and inflammation. Nat Rev Micro. 2009; 7:99–109.
23. Wiese M, Gerlach RG, Popp I, Matuszak J, Mahapatro M, Castiglione K, Chakravortty D, Willam C, Hensel M, Bogdan C, Jantsch J. Hypoxia-mediated impairment of the mitochondrial respiratory chain inhibits the bactericidal activity of macrophages. Infect. Immun. 2012; 80:1455–1466. [PubMed: 22252868]
24. Tschopp J. Mitochondria: Sovereign of inflammation? European journal of immunology. 2011; 41:1196–1202. [PubMed: 21469137]
25. Rudel T, Kepp O, Kozjak-Pavlovic V. Interactions between bacterial pathogens and mitochondrial cell death pathways. Nat Rev Micro. 2010; 8:693–705.
26. Hwang I-Y, Quan JH, Ahn M-H, Ahmed HAH, Cha G-H, Shin D-W, Lee Y-H. Toxoplasma gondii infection inhibits the mitochondrial apoptosis through induction of Bcl-2 and HSP70. Parasitol. Res. 2010; 107:1313–1321. [PubMed: 20680337]
27. Damiani G, Kiyotaki C, Soeller W, Sasada M, Peisach J, Bloom BR. Macrophage variants in oxygen metabolism. The Journal of experimental medicine. 1980; 152:808–822. [PubMed: 6252274]
28. Casadevall A, Cleare W, Feldmesser M, Glatman-Freedman A, Goldman DL, Kozel TR, Lendvai N, Mukherjee J, Pirofski LA, Rivera J, Rosas AL, Scharff MD, Valadon P, Westin K, Zhong Z. Characterization of a murine monoclonal antibody to Cryptococcus neoformans polysaccharide that is a candidate for human therapeutic studies. Antimicrobial agents and chemotherapy. 1998; 42:1437–1446. [PubMed: 9624491]
29. Franceschini A, Szklarczyk D, Frankild S, Kuhn M, Simonovic M, Roth A, Lin J, Minguez P, Bork P, Von Mering C, Jensen LJ. STRING v9.1: protein-protein interaction networks, with increased coverage and integration. Nucleic Acids Research. 2012; 41:D808–D815. [PubMed: 23203871]
30. Theill LE, Boyle WJ, Penninger JM. RANK-L and RANK: T cells, bone loss, and mammalian evolution. Annu. Rev. Immunol. 2002; 20:795–823. [PubMed: 11861618]
31. Bosco MC, Pierobon D, Blengio F, Raggi F, Vanni C, Gattorno M, Eva A, Novelli F, Cappello P, Giovarelli M, Varesio L. Hypoxia modulates the gene expression profile of immunoregulatory

receptors in human mature dendritic cells: identification of TREM-1 as a novel hypoxic marker in vitro and in vivo. Blood. 2011; 117:2625–2639. [PubMed: 21148811]

32. Buckland KF, Ramaprakash H, Murray LA, Carpenter KJ, Choi ES, Kunkel SL, Lukacs NW, Xing Z, Aoki N, Hartl D, Hogaboam CM. Triggering Receptor Expressed on Myeloid cells-1 (TREM-1) Modulates Immune Responses to Aspergillus fumigatus During Fungal Asthma in Mice. Immunol Invest. 2011; 40:692–722. [PubMed: 21592044]
33. Arora S, Olszewski MA, Tsang TM, McDonald RA, Toews GB, Huffnagle GB. Effect of Cytokine Interplay on Macrophage Polarization during Chronic Pulmonary Infection with Cryptococcus neoformans. Infect. Immun. 2011; 79:1915–1926. [PubMed: 21383052]
34. Grahl N, Dinamarco TM, Willger SD, Goldman GH, Cramer RA. Aspergillus fumigatus mitochondrial electron transport chain mediates oxidative stress homeostasis, hypoxia responses and fungal pathogenesis. Molecular microbiology. 2012; 84:383–399. [PubMed: 22443190]
35. Lischke T, Heesch K, Schumacher V, Schneider M, Haag F, Koch-Nolte F, Mittrücker H-W. CD38 controls the innate immune response against Listeria monocytogenes. Infect. Immun. 2013; 81:4091–4099. [PubMed: 23980105]
36. David A, Dolan BP, Hickman HD, Knowlton JJ, Clavarino G, Pierre P, Bennink JR, Yewdell JW. Nuclear translation visualized by ribosome-bound nascent chain puromycylation. The Journal of cell biology. 2012; 197:45–57. [PubMed: 22472439]
37. Perry SW, Norman JP, Barbieri J, Brown EB, Gelbard HA. Mitochondrial membrane potential probes and the proton gradient: a practical usage guide. Bio Techniques. 2011; 50:98–115.
38. Everts B, Amiel E, van der Windt GJW, Freitas TC, Chott R, Yarasheski KE, Pearce EL, Pearce EJ. Commitment to glycolysis sustains survival of NO-producing inflammatory dendritic cells. Blood. 2012; 120:1422–1431. [PubMed: 22786879]
39. Luo Y, Tucker SC, Casadevall A. Fc- and complement-receptor activation stimulates cell cycle progression of macrophage cells from G1 to S. Journal of immunology. 2005; 174:7226–7233.
40. Battegay EJ, Rupp J, Iruela-Arispe L, Sage EH, Pech M. PDGF-BB modulates endothelial proliferation and angiogenesis in vitro via PDGF beta-receptors. The Journal of cell biology. 1994; 125:917–928. [PubMed: 7514607]
41. Wen W, Ding J, Sun W, Wu K, Ning B, Gong W, He G, Huang S, Ding X, Yin P, Chen L, Liu Q, Xie W, Wang H. Suppression of cyclin D1 by hypoxia-inducible factor-1 via direct mechanism inhibits the proliferation and 5-fluorouracil-induced apoptosis of A549 cells. Cancer Res. 2010; 70:2010–2019. [PubMed: 20179204]
42. Zimmermann M, Arachchige-Don AS, Donaldson MS, Dallapiazza RF, Cowan CE, Horne MC. Elevated cyclin G2 expression intersects with DNA damage checkpoint signaling and is required for a potent G2/M checkpoint arrest response to doxorubicin. J Biol Chem. 2012; 287:22838–22853. [PubMed: 22589537]
43. Williams BR. PKR; a sentinel kinase for cellular stress. Oncogene. 1999; 18:6112–6120. [PubMed: 10557102]
44. Chakrabarti S, Liehl P, Buchon N, Lemaitre B. Infection-Induced Host Translational Blockage Inhibits Immune Responses and Epithelial Renewal in the Drosophila Gut. Cell host & microbe. 2012
45. Mohr I, Sonenberg N. Host Translation at the Nexus of Infection and Immunity. Cell host & microbe. 2012; 12:470–483. [PubMed: 23084916]
46. Coelho C, Bocca AL, Casadevall A. The intracellular life of Cryptococcus neoformans. Annu Rev Pathol. 2014; 9:219–238. [PubMed: 24050625]
47. Koterski JF, Nahvi M, Venkatesan MM, Haimovich B. Virulent Shigella flexneri causes damage to mitochondria and triggers necrosis in infected human monocyte-derived macrophages. Infect. Immun. 2005; 73:504–513. [PubMed: 15618190]
48. Jamwal S, Midha MK, Verma HN, Basu A, Rao KVS, Manivel V. Characterizing virulence-specific perturbations in the mitochondrial function of macrophages infected with Mycobacterium tuberculosis. Scientific reports. 2013; 3:1328. [PubMed: 23435464]
49. van der Windt GJW, O'Sullivan D, Everts B, Huang SC-C, Buck MD, Curtis JD, Chang C-H, Smith AM, Ai T, Faubert B, Jones RG, Pearce EJ, Pearce EL. CD8 memory T cells have a bioenergetic advantage that underlies their rapid recall ability. Proceedings of the National

Academy of Sciences of the United States of America. 2013; 110:14336–14341. [PubMed: 23940348]

50. Syed M, Panchal D, Joo M, Colonna M. Trem-1 Modulates Expression Of Mitofusins And Promotes Macrophage Survival. Am J Respir Crit Care Med. 2013
51. Frases S, Pontes B, Nimrichter L, Viana NB, Rodrigues ML, Casadevall A. Capsule of Cryptococcus neoformans grows by enlargement of polysaccharide molecules. Proceedings of the National Academy of Sciences of the United States of America. 2009; 106:1228–1233. [PubMed: 19164571]
52. Semenza GL. Hypoxia-inducible factor 1: regulator of mitochondrial metabolism and mediator of ischemic preconditioning. Biochim. Biophys. Acta. 2011; 1813:1263–1268. [PubMed: 20732359]
53. Beltrán B, Quintero M, García-Zaragozá E, O'Connor E, Esplugues JV, Moncada S. Inhibition of mitochondrial respiration by endogenous nitric oxide: a critical step in Fas signaling. Proc. Natl. Acad. Sci. U.S.A. 2002; 99:8892–8897. [PubMed: 12077295]
54. Ma H, May RC. Mitochondria and the regulation of hypervirulence in the fatal fungal outbreak on Vancouver Island. Virulence. 2010; 1:197–201. [PubMed: 21178442]
55. Price MS, Betancourt-Quiroz M, Price JL, Toffaletti DL, Vora H, Hu G, Kronstad JW, Perfect JR. Cryptococcus neoformans Requires a Functional Glycolytic Pathway for Disease but Not Persistence in the Host. MBio. 2011; 2 e00103-11-e00103-11.
56. Grahl N, Shepardson KM, Chung D, Cramer RA. Hypoxia and Fungal Pathogenesis: To Air or Not To Air? Eukaryotic cell. 2012; 11:560–570. [PubMed: 22447924]
57. Schaffner A, Douglas H, Braude AI, Davis CE. Killing of Aspergillus spores depends on the anatomical source of the macrophage. Infect. Immun. 1983; 42:1109–1115. [PubMed: 6642661]
58. Vogt G, Nathan C. In vitro differentiation of human macrophages with enhanced antimycobacterial activity. The Journal of clinical investigation. 2011; 121:3889–3901. [PubMed: 21911939]
59. Osterholzer JJ, Chen G-H, Olszewski MA, Zhang Y-M, Curtis JL, Huffnagle GB, Toews GB. Chemokine Receptor 2-Mediated Accumulation of Fungicidal Exudate Macrophages in Mice That Clear Cryptococcal Lung Infection. The American journal of pathology. 2011; 178:198–211. [PubMed: 21224057]
60. Casadevall A, Pirofski LA. Host-pathogen interactions: redefining the basic concepts of virulence and pathogenicity. Infect. Immun. 1999; 67:3703–3713. [PubMed: 10417127]
61. Stavru F, Palmer AE, Wang C, Youle RJ, Cossart P. Atypical mitochondrial fission upon bacterial infection. Proceedings of the National Academy of Sciences of the United States of America. 2013; 110:16003–16008. [PubMed: 24043775]
62. Sakamaki T, Casimiro MC, Ju X, Quong AA, Katiyar S, Liu M, Jiao X, Li A, Zhang X, Lu Y, Wang C, Byers S, Nicholson R, Link T, Shemluck M, Yang J, Fricke ST, Novikoff PM, Papanikolaou A, Arnold A, Albanese C, Pestell R. Cyclin D1 Determines Mitochondrial Function In Vivo. Molecular and cellular biology. 2006; 26:5449–5469. [PubMed: 16809779]
63. Casadevall A, Pirofski LA. Accidental virulence, cryptic pathogenesis, martians, lost hosts, and the pathogenicity of environmental microbes. Eukaryotic cell. 2007; 6:2169–2174. [PubMed: 17951515]
64. Stavru F, Bouillaud F, Sartori A, Ricquier D, Cossart P. Listeria monocytogenes transiently alters mitochondrial dynamics during infection. Proceedings of the National Academy of Sciences of the United States of America. 2011; 108:3612–3617. [PubMed: 21321208]

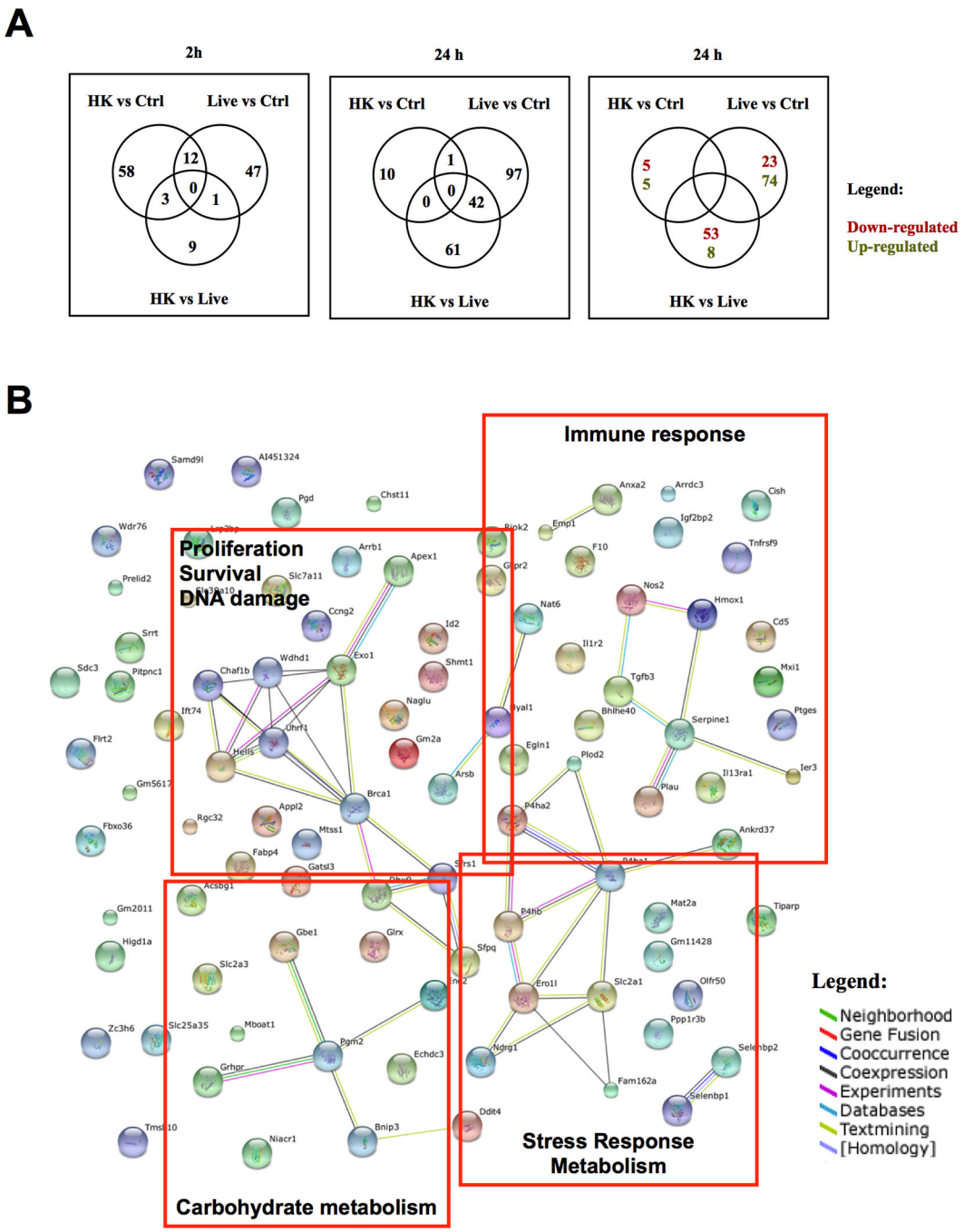

Figure 1. Gene expression changes upon infection of macrophage like J774.16 cells following opsonic ingestion of Cn

Gene expression changes in J774.16 macrophage-like cells due to their opsonic ingestion of Live Cn or heat-killed Cn (HK Cn) were analyzed. A) Venn diagrams of gene expression changes occurring in uninfected J774.16 cells (Ctrl) compared with changes occurring in Live or Heat-Killed Cn (HK) infected cells. B) STRING database illustration of reported associations between the genes that were found differentially regulated after 24 h infection with Live Cn. Orange boxes show empirical gene functional clusters. Different line colors represent types of evidence found (see legend) for the association between proteins (nodes).

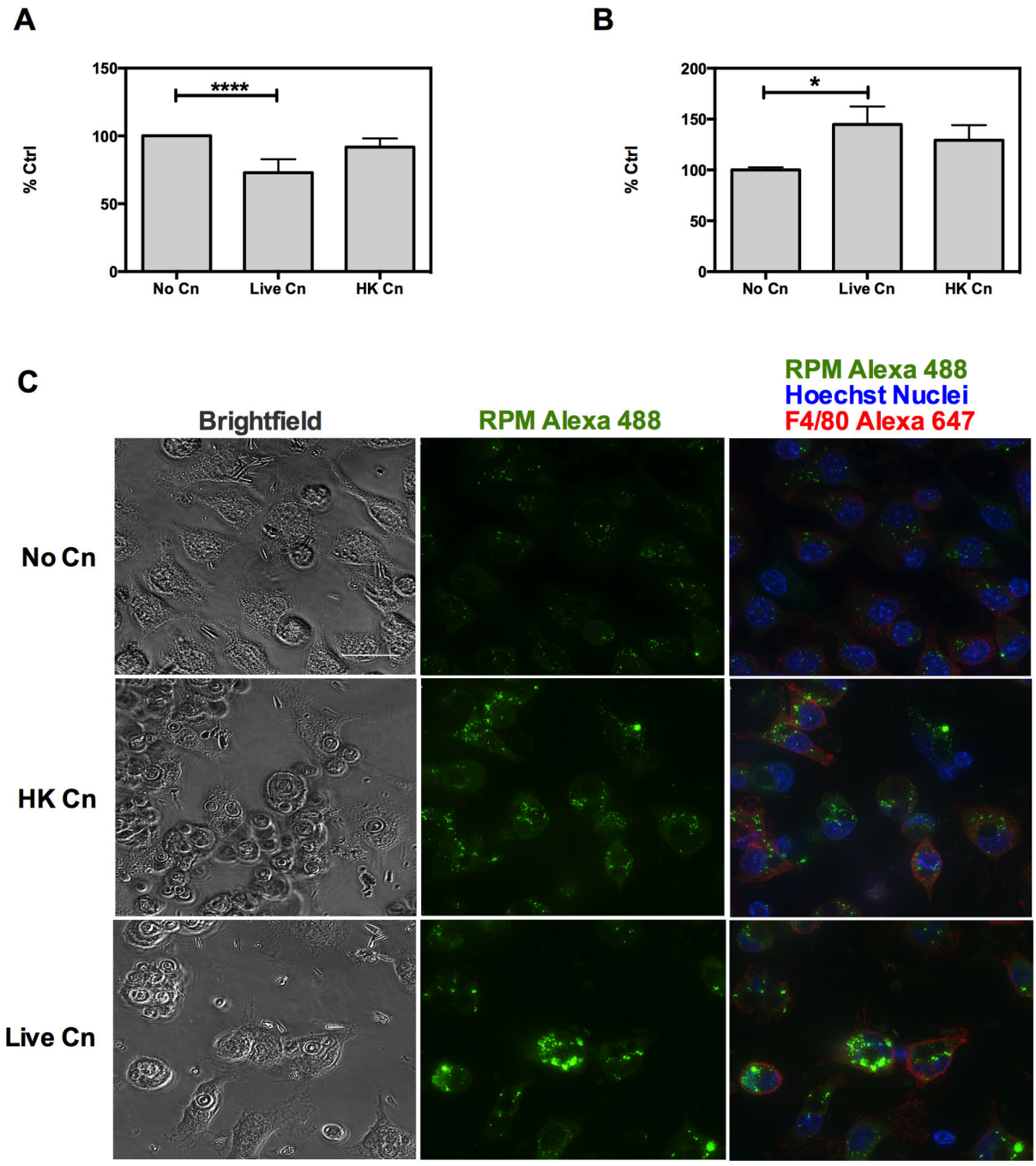

Figure 2. Cn infection of murine macrophages alters protein translation rate in host cells

Murine macrophages were infected with opsonized Live Cn or Heat-Killed Cn (HK Cn) for 24 h and protein translation was measured by RPM method as described by (David et al., 2012). RPM consists in puromycin tagging of nascent ribosomes. Amount of bound puromycin is measured by measuring puromycin-bound 2D10 antibody and it is proportional to the amount of actively translating ribosomes. Quantification of actively translating ribosomes by RPM for A) J77.16 macrophage type cells and B) Peritoneal macrophages. Experiments were repeated three times for each cell type. **** $p < 0.001$; * p

>0.05 for two-way ANOVA with Bonferroni multi comparison correction. Shown is mean and SEM of all experiments. C) Representative images of RPM staining in peritoneal macrophages. Original magnification 63× and scale bar 20 μm. Experiments were repeated three times for a minimum of 30 cells per condition per experiment and representative images are shown.

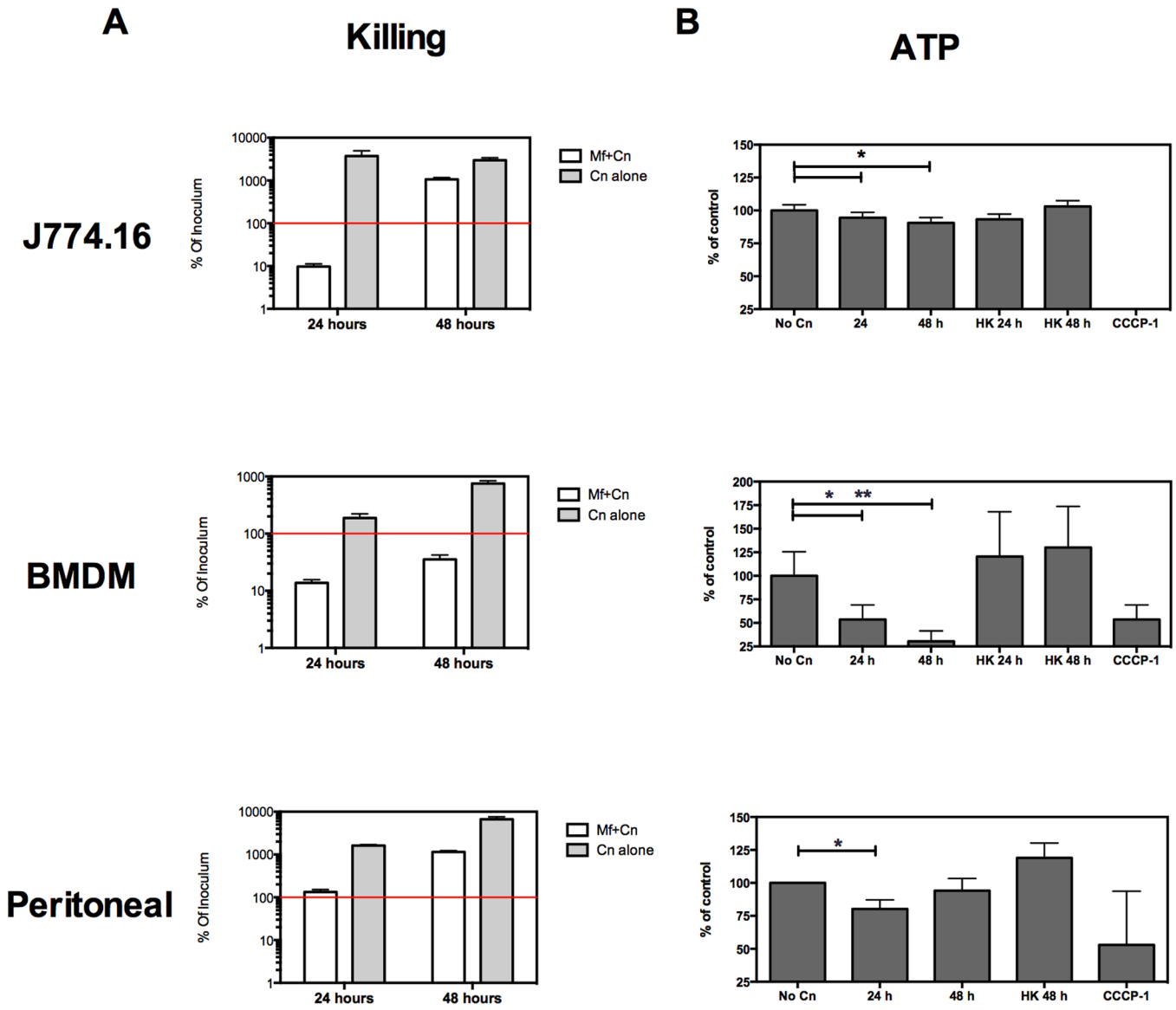

Figure 3. Murine macrophages and macrophage-like J774.16 cell line manifest reduced viability upon Cn infection and only partially restrict Cn growth *in vitro*

Murine macrophages were exposed to opsonized Cn for the indicated times. Macrophage viability was assessed by homogenate ATP levels and fungicidal activity was measured in parallel by quantifying Colony Forming Units (CFU). A) Cn growth after infection of murine macrophages. Red line indicates amount of Cn that was used to infect macrophages (initial inoculum). Experiments were repeated 2–3 times for each cell type. CFU determinations were performed in triplicate and ATP determinations in quintuplicates. B) Total ATP levels of murine macrophages after exposed to Live or Heat-killed Cn (HK Cn), normalized to ATP levels of uninfected macrophages (% of control). CCCP-1 is a positive control causing extensive cell death at 24 h. Shown is mean and SEM of all experiments for BMDM and Peritoneal macrophages. For J774.16 cells show is one representative experiment. * $p > 0.05$ for two-tailed Student's t test.

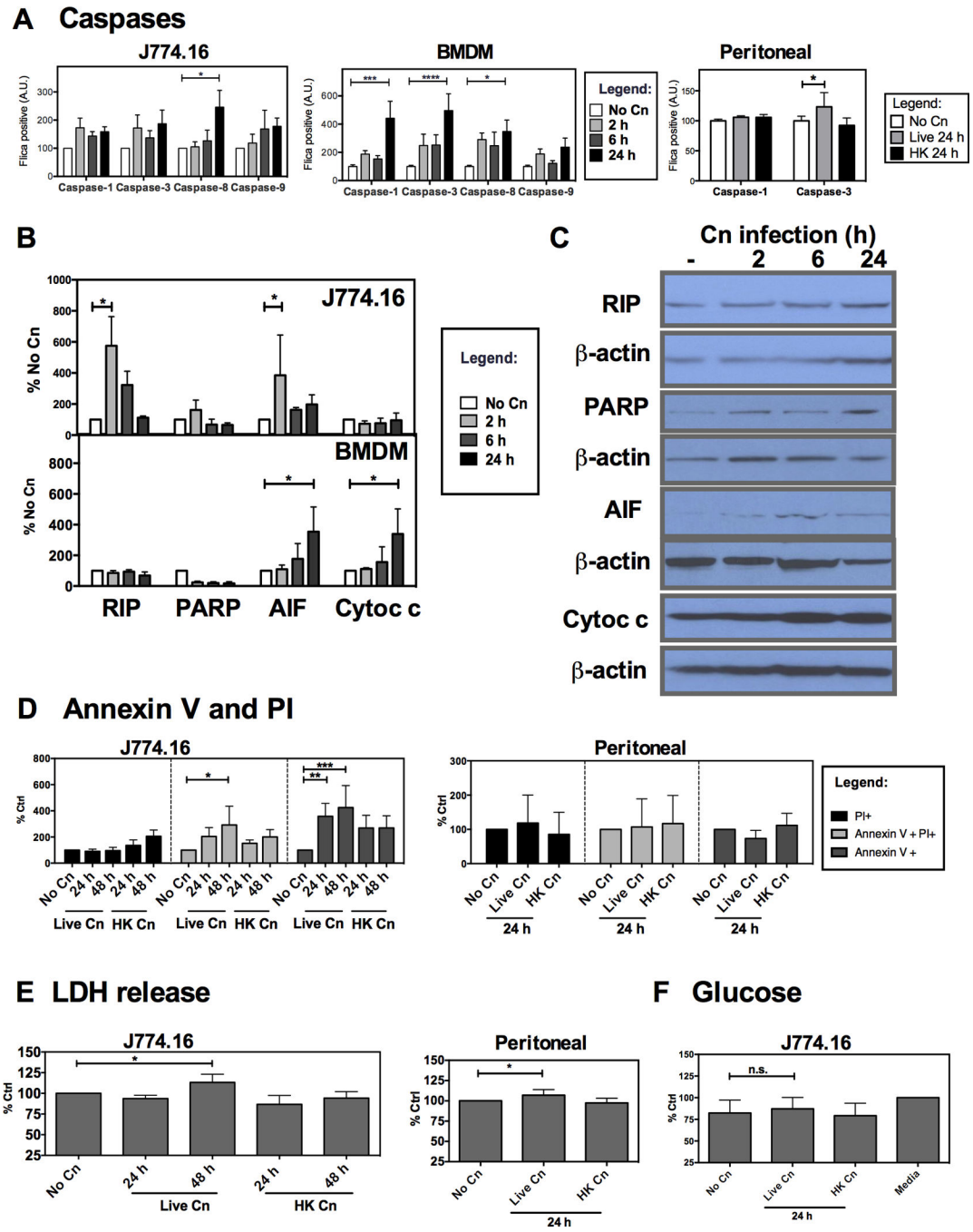

Figure 4. Programmed Cell Death Pathways are activated in murine macrophages and macrophage-like J774.16 cell line infected with Cn

Cell death in murine macrophages infected with Cn was characterized by caspase activation was measured through binding of a fluorescent caspase specific peptide (FLICA) and immunoblot quantification of molecules involved in cell death pathways. Cell death was quantified by measuring externalization of Annexin V and by release of lactate dehydrogenase (LDH) into the extracellular media. A) Measurement of caspase activation after Cn infection of J774.16 cells (left), BMDM macrophages (center) and peritoneal macrophages (right). Experiments were repeated 3–5 times for J774.16 macrophages and

BMDM with duplicate wells and twice for peritoneal macrophages. B) Quantification of protein expression for RIP, AIF, cleaved PARP and release of cytochrome c from the cytosol after infection of J774.16 and BMDM. Expression levels were normalized for β-actin content. C) Representative immunoblots for J774.16 cells. D) Quantification of Annexin V+ and PI+ cells after Cn infection of J774.16 cells (left) and peritoneal cells (right). E) LDH release for J774.16 cells (left) and peritoneal cells (right) F) Glucose quantification in cell supernatants for J774.16 cells. Experiments were repeated 3 times for each cell type. Data was normalized to % of uninfected macrophages (No Cn). * $p < 0.05$ for two-way ANOVA with Bonferroni multi-comparison correction. Shown is mean and SEM of all experiments.

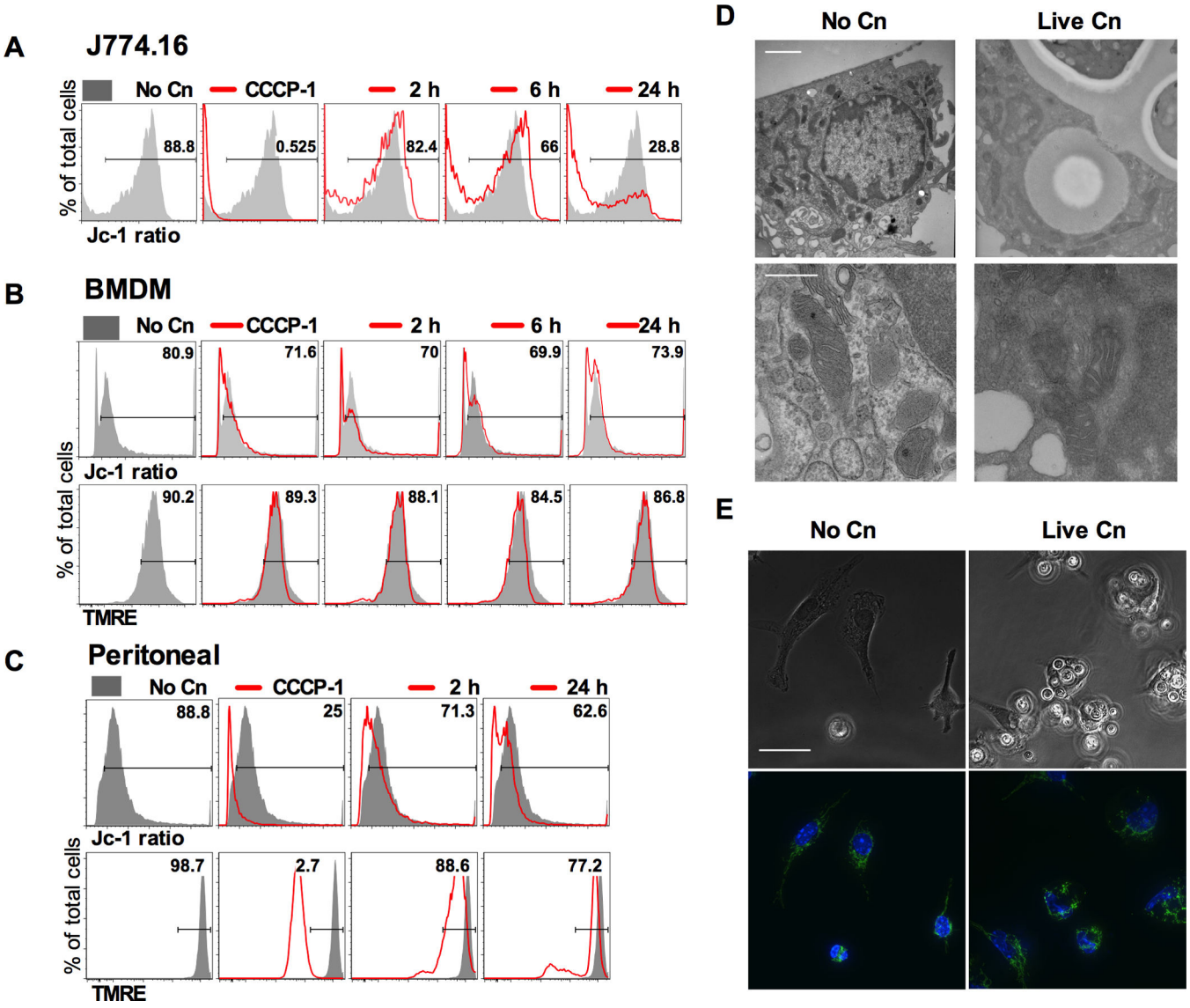

Figure 5. Murine macrophages and macrophage like J774.16 cells depolarize mitochondria after infection with Cn

Murine macrophages and macrophage like J774.16 cells were infected with opsonized Cn and their Δϕm was measured at several time intervals. CCCP-1 which causes rapid depolarization of mitochondria by uncoupling the proton gradient was used as a depolarization control. Representative histograms for A) J774.16; B) BMDM and C) Peritoneal macrophages. Numbers represent % of cells with polarized mitochondria in the experimental condition shown. Shaded grey represents non-infected macrophages (No Cn) and each experimental condition is shown by the red line. Δϕm was measured by flow cytometry analysis of the Jc-1 red/green ratio or by TMRE dye accumulation. Ratio of red/green fluorescent signal reflected mitochondrial polarization for Jc-1. TMRE accumulation is proportional to mitochondrial polarization. Experiments were repeated 2–3 times for each macrophage cell type and a representative experiment is shown. D) Mitochondrial morphology was studied by electron microscopy. No alteration of mitochondria

morphology, such as nonexistent or swollen cristae,was observed. Scale bar 500 nm and bottom row is magnification of mitochondria on top row. E) Peritoneal macrophages infected with Cn show fragmented mitochondrial network, as inferred by cytochrome c immunostaining (green) was altered by the presence of Cn. Images were counterstained with Hoechst nuclear dye (blue). Original magnification 63× and scale bar 50 μm. Experiments were repeated three times and representative images are shown.

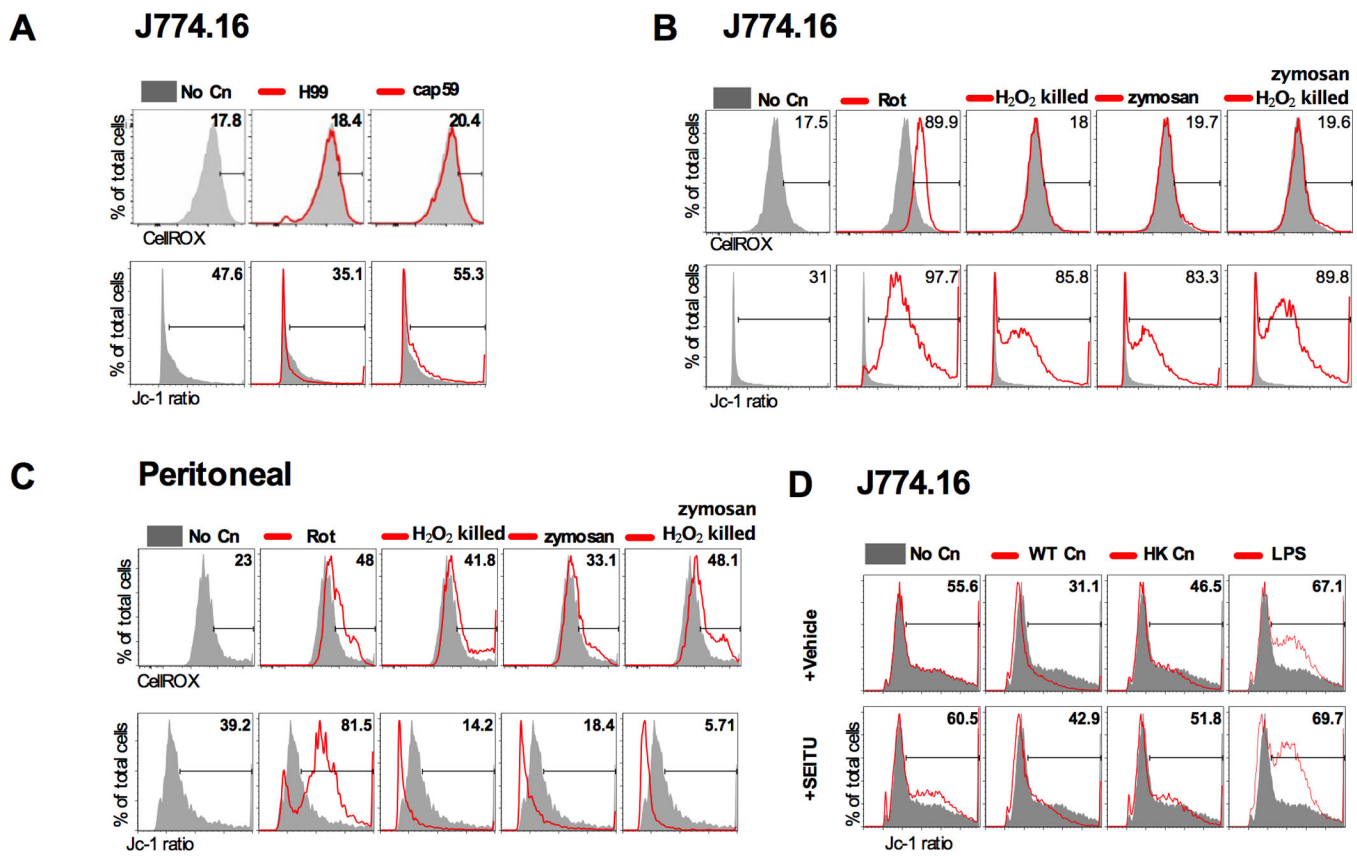

Figure 6. Mitochondrial alterations do not correlate with oxidative burst but are mediated by NO

Peritoneal macrophages but not J774.16 macrophage-like cells produced ROS upon Cn infection. However pattern of ROS production did not follow the pattern of mitochondrial depolarization suggesting non mitochondrial derived ROS. As a positive control we used rotenone (Rot) which blocks mitochondrial respiratory chain, resulting in accumulation of electrons, hyperpolarization and increase in cellular ROS. A) J774.16 cells were infected for 24 h with either H99 or an acapsular strain (cap59). B) J774.16 were exposed to opsonized H_2O_2 killed Cn or zymosan, resulting in mitochondrial hyperpolarization but no ROS production. C) Peritoneal cells were exposed to opsonized H_2O_2 killed Cn or zymosan resulting in $\Delta\phi m$ decrease and abundant ROS. D) Addition of 500 μM of SEITU prevented mitochondrial depolarization in peritoneal macrophages and J774.16 cells (not shown). Total ROS were measured by CellROX® Deep Red Reagent and $\Delta\phi m$ was measured by the ratio of Jc-1 red/green fluorescence, using flow cytometry. Numbers represent % of cells within each region. Shaded grey represents non-infected macrophages (No Cn) and each experimental condition is shown by the red line. Each experiment was repeated twice for both J774.16 cells and peritoneal macrophages. Shown are plots of representative experiments.

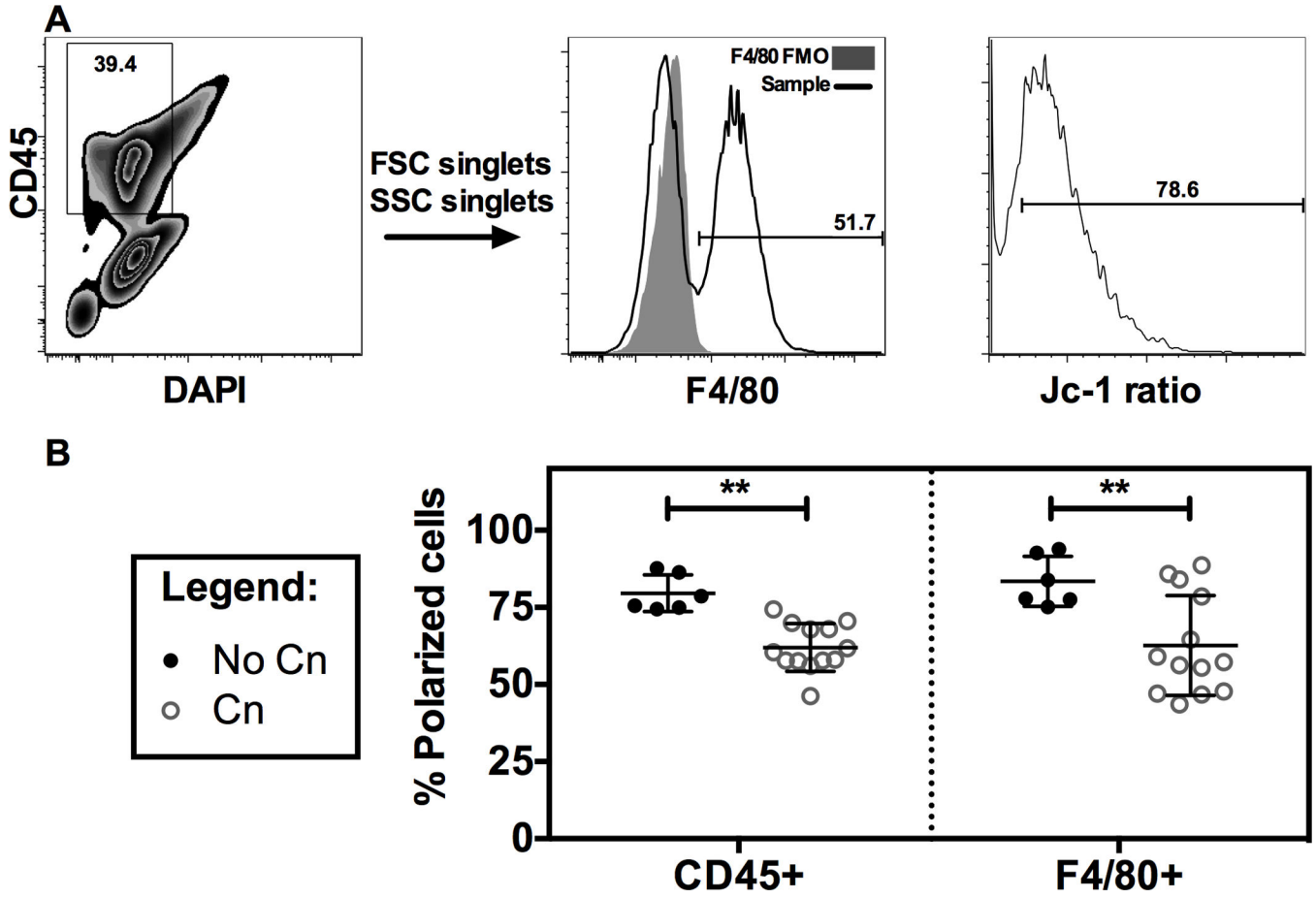

Figure 7. Intraperitoneal infection of mice with Cn causes a decrease in mitochondrial polarization in peritoneal total leukocytes and macrophages

C57/B6 mice were infected with Cn i.p and after 24 hours peritoneal lavage cells had decreased Δϕm. A) Flow cytometry gating strategy for evaluating Δϕm in peritoneal lavage CD45+ (total leukocytes) and F4/80+ (macrophages) cells. Shaded area shows the fluorescence minus one (F4/80 FMO) tube, used as negative control. B) Quantification of Δϕm in peritoneal lavage cells infected with Cn for 24 h. Jc-1 dye was injected in the peritoneum to measure Δϕm *in vivo*. Peritoneal lavage was performed and cells immunostained for CD45 and F4/80 in a flow cytometer. Experiments were performed twice and each data point represents 1 mouse, with a total of 6 mice in No Cn and 13 mice for Cn for both experiments. Also shown is mean and SD. ** $p < 0.01$ for two-way ANOVA with Bonferroni correction.

Table 1

Summary of findings

	J774.16 macrophage like	BMDM	Peritoneal macrophages
Fungal Control	++	++	+
ATP Levels	↓	↓↓	↓↓
PCD pathways			
LDH release	Yes	No	Yes
Annexin V binding	Yes	N.D.[2]	Yes
Activation of:			
Caspases	−8	−1, −3, −8	−3
RIP	Yes	No	N.D.[1]
AIF	Yes	Yes	N.D.[1]
PARP	No	No	N.D.[1]
Release of cytochrome c	No	Yes	N.D.[1]
Predicted PCD activated	*Necrosis*	*Apoptosis*	*Apoptosis/Necrosis*
Gene expression	Stress pathways activated		
Mitochondrial characteristics			
Depolarization	++	+	++
Morphology	Fragmented	Unchanged	Fragmented
ROS Production	No	No	Yes
Mitochondrial derived ROS	No	No	No
NO-dependence	Yes	N.D.[2]	Yes
Protein translation	↓	N.D.[2]	↑

N.D.[1] not performed due to technical limitations

N.D.[2] not pertinent for conclusions of study